https://doi.org/10.5194/hess-2022-298
Preprint. Discussion started: 17 October 2022
© Author(s) 2022. CC BY 4.0 License.

Hydrology and Earth System Sciences
Open Access
Discussions

Technical note: Displacement variance of a solute particle in heterogeneous confined aquifers with random aquifer thickness fields

Ching-Min Chang[1], Chuen-Fa Ni[1], Chi-Ping Lin[2], and I-Hsien Lee[2]

[1]Graduate Institute of Applied Geology, National Central University, Taoyuan, Taiwan

[2]Center for Environmental Studies, National Central University, Taoyuan, Taiwan

Correspondence: Chuen-Fa Ni (nichuenfa@geo.ncu.edu.tw)

https://doi.org/10.5194/hess-2022-298
Preprint. Discussion started: 17 October 2022
© Author(s) 2022. CC BY 4.0 License.

Abstract. In this work, the problem of regional-scale transport of inert solutes in heterogeneous confined aquifers of variable thickness is analyzed in a stochastic framework. A general stochastic methodology for deriving the variance of the displacement of a solute particle is given based on the two-dimensional depth-averaged solute mass conservation equation and the Fokker-Planck equation. The variability in solute displacement is attributed to the variability in hydraulic conductivity and aquifer thickness. Explicit results for the solute displacement variance in the mean flow direction are obtained assuming that the fluctuations in log hydraulic conductivity and log thickness of the confined aquifer are second-order stationary processes. The results show that variation in hydraulic conductivity and aquifer thickness can lead to nonstationarity in the covariance of flow velocity, making longitudinal macrodispersion anomalous and increasing linearly with travel time at large distances.

1 Introduction

It is widely accepted that the variability of solute movement in heterogeneous aquifers is controlled primarily by the spatial variability of groundwater flow fields (e.g., Dagan, 1989; Gelhar, 1993; Rubin, 2003). Much work on the stochastic analysis of solute transport in heterogeneous porous formations has focused on relating the spatial variability of the hydraulic conductivity field to that of the flow velocity field, and thus to the spatial variability of the displacement of a solute particle. However, natural aquifers at regional scales often exhibit nonuniform aquifer thickness (e.g., Masterson et al., 2013; Zamrsky et al., 2018; DeSimone et al., 2020), and spatial variability in the aquifer thickness field has also been shown to have an important influence on flow field variability (e.g., Hantush, 1962; Cuello and Guarracino, 2020; Chang et al., 2021). Thus, the underlying motivation for this work is to provide an analytical stochastic method for improved quantification of the variability of solution displacement at the regional scale in heterogeneous aquifers under more realistic field conditions, i.e., taking into account the effects not only of the spatial variation of the hydraulic conductivity field but also of the thickness field of the confined aquifer.

At a regional scale, the lateral extent of the confined aquifer is much greater than the thickness of the formation. Therefore, it is more practical to view the flow and solute transport processes in confined aquifers at the regional scale as essentially two-dimensional, areal processes. In the traditional approach to the essentially horizontal flow, the stochastic description of flow and solute transport processes is related to the stochastic properties of transmissivity (e.g., Dagan, 1982; 1984), where

https://doi.org/10.5194/hess-2022-298
Preprint. Discussion started: 17 October 2022
© Author(s) 2022. CC BY 4.0 License.
Hydrology and Earth System Sciences
Open Access
Discussions

the transmissivity is the line integration of hydraulic conductivity over the depth of the formation at a given point. However, in reality, transmissivity measurements from field tests give a value of integrated hydraulic conductivity over a larger volume than the range used for the line integration of hydraulic conductivity at a single point. This means that the field tests performed for the transmissivity measurements include more of the heterogeneity in the formation than that encountered over the depth of the formation at a single point. This would result in a reduction in the variance of transmissivity and an overestimation of the integral scale of transmissivity compared to values predicted from the line integration of hydraulic conductivity. Consequently, using the stochastic properties of transmissity may not provide an accurate interpretation of solute movement at a regional scale.

Rather than using the stochastic properties of transmissity, this work uses the stochastic properties of hydraulic conductivity and thickness of the confined aquifer to interpret the variability of solute movement at a regional scale using a hydraulic approach (or essentially horizontal flow approach) (Bear, 1979; Bear and Cheng, 2010). That is, in this approach, the variability in solute movement is due to variations in hydraulic conductivity and aquifer thickness. In the present work, a general stochastic methodology is developed to describe the variability of regional-scale solute transport, e.g., the variance of solute displacement, based on the

© Author(s) 2022. CC BY 4.0 License.

two-dimensional depth-averaged solute mass conservation equation and the Fokker-Planck equation. Explicit results for the displacement variance in the mean flow direction are obtained for the case where the random fields of log conductivity and log thickness of the confined aquifer are second-order stationary. To our knowledge, variation in hydraulic conductivity and aquifer thickness have not previously been used as driving forces to quantify the variability of solute movement in essentially horizontal flow fields. The stochastic theory presented here improves quantification of the variance of the solute displacement in natural confined aquifers of random thickness fields.

2 Mathematical formulation of the problem

Consider here the steady flow of a fluid carrying an inert solute through a heterogeneous confined aquifer with variable thickness. When the dispersion tensor is expressed in its three principal directions and these principal directions are used as Cartesian coordinate axes, the equation for the transport of inert solutes through a rigid, saturated porous medium is (e.g., de Marsily, 1986)

$$n\frac{\partial c}{\partial t}=\frac{\partial}{\partial x_i}[D_i\frac{\partial c}{\partial x_i}-cq_i] \qquad i=1,2,3, \tag{1}$$

where n is the porosity, c is the solute concentration, and D_i and q_i are the dispersion

https://doi.org/10.5194/hess-2022-298
Preprint. Discussion started: 17 October 2022
© Author(s) 2022. CC BY 4.0 License.

Hydrology and Earth System Sciences
Open Access
Discussions

coefficient and the specific discharge in the x_i direction, respectively. In the case where the constituents are well mixed across the thickness of the aquifer (flow depth), it is convenient to define the depth-averaged concentration in the x_1 and x_2 directions.

Integrating Eq. (1) with respect to x_3 over the vertical thickness of a confined aquifer, $B(x_1, x_2)$, together with Leibniz's rule and no-slip condition for the dispersive and diffusive fluxes at upper and lower boundaries of the confined aquifer, yields the two-dimensional, depth-averaged equation for conservation of solute mass (e.g., Holly, 1975; Fischer et al., 1979)

$$\frac{\partial}{\partial t}[B\tilde{c}] = \frac{\partial}{\partial x_i}\left[\frac{\tilde{D}_i}{n} B \frac{\partial \tilde{c}}{\partial x_i}\right] - \frac{\partial}{\partial x_i}\left[\frac{\tilde{q}_i}{n} B\tilde{c}\right] \qquad i = 1,2, \tag{2}$$

where $\tilde{D}_i$, $\tilde{c}$, and $\tilde{q}_i$ represent the depth-averaged dispersion coefficient, depth-averaged solute concentration, and depth-averaged specific discharge, respectively. Starting from the identity,

$$\begin{aligned} \frac{\tilde{D}_i}{n} B \frac{\partial \tilde{c}}{\partial x_i} &= \frac{\partial}{\partial x_i}\left[\frac{\tilde{D}_i}{n} B\tilde{c}\right] - \tilde{c}\frac{\partial}{\partial x_i}\left[\frac{\tilde{D}_i}{n} B\right] \\ &= \frac{\partial}{\partial x_i}\left[\frac{\tilde{D}_i}{n} B\tilde{c}\right] - B\tilde{c}\frac{1}{n}\frac{\partial \tilde{D}_i}{\partial x_i} - \frac{\tilde{D}_i}{n} B\tilde{c}\frac{\partial \ln B}{\partial x_i} \qquad i = 1,2, \end{aligned} \tag{3}$$

Eq. (2) can be rewritten as follows:

$$\frac{\partial}{\partial t}[B\tilde{c}] = \frac{\partial^2}{\partial x_i^2}\left[\frac{\tilde{D}_i}{n} B\tilde{c}\right] - \frac{\partial}{\partial x_i}\left[\left(\frac{1}{n}\frac{\partial \tilde{D}_i}{\partial x_i} + \frac{\tilde{D}_i}{n}\frac{\partial \ln B}{\partial x_i} + \frac{\tilde{q}_i}{n}\right) B\tilde{c}\right] \qquad i = 1,2, \tag{4}$$

which corresponds to the form of the Fokker-Planck equation (e.g., Risken, 1989).

The concentration field associated with the solute particle can be written as (Fischer et al., 1979; Dagan, 1989)

https://doi.org/10.5194/hess-2022-298
Preprint. Discussion started: 17 October 2022
© Author(s) 2022. CC BY 4.0 License.

$$B\tilde{c} = \frac{M}{n} f(\boldsymbol{x};t,\boldsymbol{a},t_0), \tag{5}$$

where M is the solute mass, $f(\boldsymbol{x};t,\boldsymbol{a},t_0)$ stands for the probability density function of the particle displacement which originates at $\boldsymbol{x} = \boldsymbol{a}$ for $t = t_0$. Substituting Eq. (5) into Eq. (4) gives

$$\frac{\partial}{\partial t} f(\boldsymbol{x};t) = \frac{\partial^2}{\partial x_i^2}\left[\frac{\tilde{D}_i}{n} f(\boldsymbol{x};t)\right] - \frac{\partial}{\partial x_i}\left[\left(\frac{1}{n}\frac{\partial \tilde{D}_i}{\partial x_i} + \frac{\tilde{D}_i}{n}\frac{\partial \ln B}{\partial x_i} + \frac{\tilde{q}_i}{n}\right) f(\boldsymbol{x};t)\right] \qquad i = 1,2, \tag{6}$$

which is known as the Fokker-Planck equation. Moreover, it can be shown that the stochastic differential equation for the evolution of stochastic process (e.g., Van Kampen, 1992; Jing et al., 2019)

$$\frac{dX_i}{dt} = \mu_i(\boldsymbol{X}(t)) + \sigma_i(\boldsymbol{X}(t))\frac{dW}{dt} \qquad i = 1,2, \tag{7}$$

where $\boldsymbol{X}(= (X_1,X_2))$ is the displacement, μ_i is the drift coefficient, σ_i is the diffusion coefficient, and W denotes a Wiener process, is equivalent to the Fokker-Planck equation (6) such that

$$\mu_i = \frac{1}{n}\frac{\partial}{\partial X_i}\tilde{D}_i(\boldsymbol{X}) + \frac{1}{n}\tilde{D}_i(\boldsymbol{X})\frac{\partial}{\partial X_i}\ln B(\boldsymbol{X}) + \frac{1}{n}\tilde{q}_i(\boldsymbol{X}) \qquad i = 1,2, \tag{8a}$$

$$\sigma_i^2 = \frac{2}{n}\tilde{D}_i(\boldsymbol{X}) \qquad i = 1,2, \tag{8b}$$

This means,

$$\frac{dX_i}{dt} = \left[\frac{1}{n}\frac{\partial}{\partial X_i}\tilde{D}_i(\boldsymbol{X}) + \frac{1}{n}\tilde{D}_i(\boldsymbol{X})\frac{\partial}{\partial X_i}\ln B(\boldsymbol{X}) + \frac{1}{n}\tilde{q}_i(\boldsymbol{X})\right] + \sqrt{\frac{2}{n}\tilde{D}_i(\boldsymbol{X})}\frac{dW}{dt} \qquad i = 1,2. \tag{9}$$

In this study, the fields (or processes) of hydraulic conductivity $K(x_1,x_2)$ and thickness of the confined aquifer $B(x_1,x_2)$ are considered spatially random. It is also assumed that the mean fluid flow is uniform and unidirectional in the x_1-direction, i.e.,

https://doi.org/10.5194/hess-2022-298
Preprint. Discussion started: 17 October 2022
© Author(s) 2022. CC BY 4.0 License.
Hydrology and Earth System Sciences
Open Access
EGU
Discussions

the gradient of the mean depth-averaged hydraulic head $\tilde{h}$ in the x_1-direction is constant,

$$\frac{d<\tilde{h}>}{dx_1}=-J\,, \tag{10}$$

and zero in the x_2-direction, which is consistent with the result of the perturbation approach from the solution of the differential equation for the depth-averaged hydraulic head (Chang et al., 2021). Thus, $<\boldsymbol{X}> = (<X_1>, 0)$ and the depth-averaged dispersion coefficients in Eq. (9) become constant, $\tilde{D}_1 = D_L$ and $\tilde{D}_2 = D_T$.

By analogy with Butera and Tanda (1999), the expansion of Eq. (9) in Taylor series around $<\boldsymbol{X}>$ in the x_1-direction yields

$$\frac{dX_1}{dt}=\frac{1}{n}D_L\Big[\frac{d\Phi(<\boldsymbol{X}>)}{dX_1}+\frac{d^2\Phi(<\boldsymbol{X}>)}{dX_1^2}X_1^{'}+\frac{d\beta(<\boldsymbol{X}>)}{dX_1}\Big]+<\tilde{v}_1>(<\boldsymbol{X}>)+v_1<\boldsymbol{X}>+\sqrt{\frac{2}{n}D_L}\frac{dW}{dt}\,, \tag{11}$$

where $X_1^{\prime} = X_1 - <X_1>$, $\Phi = <\ln B>$, $\beta = \ln B - <\ln B>$, $v_1 = \tilde{v}_1 - <\tilde{v}_1>$, and $\tilde{v}_1 = \tilde{q}_1/n$. Note that due to the assumption of uniform mean flow in the x_1-direction, the term

$$\frac{d<\tilde{v}_1>(<\boldsymbol{X}>)}{dX_1}X_1^{'}, \tag{12}$$

has been removed from Eq. (11). Equation (11) reveals that

$$\frac{d<X_1>}{dt}=\frac{1}{n}D_L\frac{d\Phi(<\boldsymbol{X}>)}{dX_1}+<\tilde{v}_1>(<\boldsymbol{X}>)\,, \tag{13}$$

$$\frac{dX_1^{'}}{dt}-\frac{D_L}{n}\frac{d^2\Phi(<\boldsymbol{X}>)}{dX_1^2}X_1^{'}=\frac{D_L}{n}\frac{d\beta(<\boldsymbol{X}>)}{dX_1}+v_1<\boldsymbol{X}>+\sqrt{\frac{2}{n}D_L}\frac{dW}{dt}\,. \tag{14}$$

Equations (13) and (14) describe the mean and fluctuation, respectively, of the displacement of the solute particles. By the solution of Eq. (14), the variance of the solute displacement in the x_1-direction (the mean flow direction) can be evaluated in

https://doi.org/10.5194/hess-2022-298
Preprint. Discussion started: 17 October 2022
© Author(s) 2022. CC BY 4.0 License.
Hydrology and Earth System Sciences
Discussions

the frame, (e.g., Dagan, 1984; 1989)

$$X_{11}(t) = < X_1^{'}(t) X_1^{'}(t) > . \tag{15}$$

This first-order approximation for representing the head perturbation, and hence the solute displacement perturbation, should be applied to porous formations where the standard deviation of the random fluctuations of the log conductivity is less than 1. However, Zhang and Winter (1999) report in a Monte Carlo simulation study that it is accurate for the solutions of the head moment for the value of the variance of the log conductivity of up to 4.38. A similar finding from comparing moments of hydraulic head with results of numerical Monte Carlo simulations is also reported in Guadagnini and Neuman (1999) for highly heterogeneous media with a variance of log conductivity from 2 to 4.

For the case of the aquifer thickness which is a slowly spatial varying process, the term in Eq. (14), $d^2\Phi/dX_1^2$, may be neglected, and, consequently, Eq. (14) reduces to

$$\frac{dX_1^{'}}{dt} = \frac{D_L}{n}\frac{d\beta(<\mathbf{X}>)}{dX_1} + v_1 < \mathbf{X} > + \sqrt{\frac{2}{n}D_L}\frac{dW}{dt} . \tag{16}$$

Equation (16) illustrates that the variability of the particle displacement is determined by the gradient of the variation of the aquifer thickness fields, the variability of the flow velocity and the local pore-scale dispersion. Note that when flowing through a confined aquifer with variable thickness, the variability in flow velocity is influenced by both the variation in log conductivity and log thickness fields (Chang et al., 2021).

https://doi.org/10.5194/hess-2022-298
Preprint. Discussion started: 17 October 2022
© Author(s) 2022. CC BY 4.0 License.

Equations (15) and (16) form a basis of this study for the development of the displacement variance in the mean flow direction.

Since the variance of solute displacement in the x_1-direction cannot be calculated without knowing the statistics of the flow fields. Therefore, in the following section, the statistics of the flow field are developed for the case where both the variations in hydraulic conductivity and the thickness of the confined aquifer are considered to be second-order stationary processes.

3 Statistics of the flow fields

Chang et al. (2021) develop the differential equations for the flow fields (Eqs. (6) and (12) of Chang et al., 2021) in a confined aquifer with variable thickness based on a hydraulic approach to flow in aquifers (Bear, 1979; Bear and Cheng, 2010). On this basis, under the condition of steady-state flow, the equations for the depth-averaged hydraulic head and the depth-averaged specific discharge about the mean, keeping only first-order terms in the perturbations, take the following form

$$\frac{\partial^2 h}{\partial x_i^2} = J\left[\frac{\partial y}{\partial x_1} + 2\frac{\partial \beta}{\partial x_1}\right] \qquad i=1,2, \tag{17}$$

$$q_i = \bar{q}\left[(y+\beta)\delta_{1i} - \frac{1}{J}\frac{\partial h}{\partial x_i}\right] \qquad i=1,2, \tag{18}$$

where $h=\tilde{h}-<\tilde{h}>$, y = ln$K$-Y, $Y = <\ln K>$, $\beta = \ln B - <\ln B>$, $q_i=\tilde{q}_i-<\tilde{q}_i>$, and

https://doi.org/10.5194/hess-2022-298
Preprint. Discussion started: 17 October 2022
© Author(s) 2022. CC BY 4.0 License.

Hydrology and Earth System Sciences
Open Access
Discussions

$\overline{q} = <\tilde{q}_1> = e^Y J$. Equation (17) quantifies the change in depth-averaged head in response to changes in hydraulic conductivity and aquifer thickness.

Due to the property of the linearity of the driving forces, Eq. (17) can alternatively be divided into two parts as

$$\frac{\partial^2 h_y}{\partial x_i^2} = J \frac{\partial y}{\partial x_1} \qquad i = 1,2, \tag{19a}$$

$$\frac{\partial^2 h_\beta}{\partial x_i^2} = 2J \frac{\partial \beta}{\partial x_1} \qquad i = 1,2, \tag{19b}$$

where h = h_y+h_β. Equation (19) is a stochastic differential equation in which the variation in log-hydraulic conductivity (or in log-aquifer thickness) appears as a forcing term that produces the variations in depth-averaged head.

Matheron (1973) shows that if the random input process of the Poission equation is second-order stationary, then the Poission equation has a first-order intrinsic random function (1-IRF) as its solution. Since the processes y and β are second-order stationary, it can be shown that the derivatives of the processes y and β with respect to x_1 are also stationary. This means that Eq. (19) has a 1-IRF solution for h_y and h_β which admits the Fourier-Stieltjes representation as follows:

$$h_y(x_1, x_2) = J \int_{-\infty}^{\infty}\int_{-\infty}^{\infty} iR_1 \frac{1 - \exp[i(R_1x_1 + R_2x_2)] + i(R_1x_1 + R_2x_2)}{R_1^2 + R_2^2} dZ_y(R_1, R_2), \tag{20a}$$

$$h_\beta(x_1, x_2) = 2J \int_{-\infty}^{\infty}\int_{-\infty}^{\infty} iR_1 \frac{1 - \exp[i(R_1x_1 + R_2x_2)] + i(R_1x_1 + R_2x_2)}{R_1^2 + R_2^2} dZ_\beta(R_1, R_2). \tag{20b}$$

https://doi.org/10.5194/hess-2022-298
Preprint. Discussion started: 17 October 2022
© Author(s) 2022. CC BY 4.0 License.

where R_1 and R_2 are the components of the wave number vector $\boldsymbol{R}$ (= (R_1, R_2)), and Z_y and Z_β are complex-valued distributions with uncorrelated increments on wave number space. Note that a 1-IRF is the second integral of a zero-mean spatial random function (Chile`s and Delfiner, 1999).

It follows from Eq. (18) that if processes y and β are statistically independent, the covariance function for the depth-averaged flow velocity process can be evaluated with the spectral representation as follows:

$$\frac{<v_i(\xi)v_j(\zeta)>}{V^2}=[C_{yy}(\xi,\zeta)+C_{\beta\beta}(\xi,\zeta)]\delta_{1i}\delta_{1j}-\frac{1}{J}\frac{\partial}{\partial\zeta_j}[C_{yh_y}(\xi,\zeta)+C_{\beta h_\beta}(\xi,\zeta)]\delta_{1i}$$

$$-\frac{1}{J}\frac{\partial}{\partial\xi_i}[C_{yh_y}(\zeta,\xi)+C_{\beta h_\beta}(\zeta,\xi)]\delta_{1j}--\frac{1}{J^2}\frac{\partial\gamma_h(\xi,\zeta)}{\partial\xi_i\partial\zeta_j}, \quad (21)$$

where $V=\bar{q}/n=e^{Y}J/n$, ξ = (ξ_1,ξ_2), ζ = (ζ_1,ζ_2), C_{yy} and $C_{\beta\beta}$ are the ln$K$ and ln$B$ covariance functions, respectively, C_{yh_y} is the covariance of ln$K$ process with the head process, $C_{\beta h_\beta}$ is the covariance of ln$B$ process with the head process, and γ_h is the semivariogram of the head process, defined as

$$\gamma_h(\xi,\zeta)=\gamma_{h_y}(\xi,\zeta)+\gamma_{h_\beta}(\xi,\zeta)=\frac{1}{2}\left\{<[h_y(\xi)-h_y(\zeta)]^2>+<[h_\beta(\xi)-h_\beta(\zeta)]^2>\right\}. \quad (22)$$

4 Results and discussion

To determine the covariance of flow velocity, and thus the variance of solute displacement, it is assumed that the hydraulic conductivity and the thickness of the

https://doi.org/10.5194/hess-2022-298
Preprint. Discussion started: 17 October 2022
© Author(s) 2022. CC BY 4.0 License.

aquifer fields are lognormally distributed and characterized by the isotropic exponential covariance, i.e. (e.g., Dagan, 1984; Gelhar, 1993; Bailey and Baù, 2012)

$$C_{yy}(\xi,\zeta)=\sigma_y^2\exp[-\frac{|\xi-\zeta|}{\lambda_y}], \tag{23a}$$

$$C_{\beta\beta}(\xi,\zeta)=\sigma_\beta^2\exp[-\frac{|\xi-\zeta|}{\lambda_\beta}], \tag{23b}$$

where σ_y^2 and σ_β^2 are the variances of y and β, respectively, λ_y and λ_β are the integral scales of ln$K$ and ln$B$ fields, respectively. The corresponding spectra, which result from the inverse Fourier transform of Eq. (23), are as follows:

$$S_{yy}(R_1,R_2)=\frac{\sigma_y^2}{2\pi}\frac{\lambda_y^2}{[1+\lambda_y^2(R_1^2+R_2^2)]^{3/2}}, \tag{24a}$$

$$S_{\beta\beta}(R_1,R_2)=\frac{\sigma_\beta^2}{2\pi}\frac{\lambda_\beta^2}{[1+\lambda_\beta^2(R_1^2+R_2^2)]^{3/2}}. \tag{24b}$$

4.1 Covariance of flow velocity in the x_1-direction

The stationarity of the ln$K$ process allows the Fourier-Stieltjes representations (e.g., Lumley and Panofsky, 1964)

$$y(x_1,x_2)=\int_{-\infty}^{\infty}\int_{-\infty}^{\infty}\exp[i(R_1x_1+R_2x_2)]dZ_y(R_1,R_2). \tag{25}$$

Using this and Eqs. (20a) and (24a), the covariance of ln$K$ process with the head process C_{yh} in Eq. (21) is given as

$$C_{yh_y}(\xi,\zeta)=\langle y(\xi)h_y(\zeta)\rangle$$

https://doi.org/10.5194/hess-2022-298
Preprint. Discussion started: 17 October 2022
© Author(s) 2022. CC BY 4.0 License.

$$= -J \int_{-\infty}^{\infty}\int_{-\infty}^{\infty} i \frac{R_1}{R_1^2 + R_2^2} \exp[i(R_1\xi_1 + R_2\xi_2)] \{1 - \exp[-i(R_1\zeta_1 + R_2\zeta_2)] - i(R_1\zeta_1 + R_2\zeta_2)\}$$

$$\times \frac{\sigma_y^2}{2\pi} \frac{\lambda_y^2}{[1 + \lambda_y^2(R_1^2 + R_2^2)]^{3/2}} dR_1 dR_2$$

$$= \sigma_y^2 \lambda_y J[\Theta_1(\frac{\xi_1}{\lambda_y}, \frac{\xi_2}{\lambda_y}) - \frac{\zeta_1}{\lambda_y}\Theta_2(\frac{\xi_1}{\lambda_y}, \frac{\xi_2}{\lambda_y}) + \frac{\zeta_2}{\lambda_y}\Theta_3(\frac{\xi_1}{\lambda_y}, \frac{\xi_2}{\lambda_y}) - \Theta_1(\frac{\rho_1}{\lambda_y}, \frac{\rho_2}{\lambda_y})], \tag{26}$$

where $\rho_1 = \xi_1\text{-}\zeta_1$, $\rho_2 = \xi_2\text{-}\zeta_2$, and the description for the functions Θ_1-Θ_3, respectively, can be found in Appendix A. Similarly, the closed-form expression for the covariance of ln$B$ process with the head process $C_{\beta h_\beta}$ in Eq. (21) can be obtained using Eqs. (20b), (24b), and the Fourier-Stieltjes representations for the stationary ln$B$ process

$$\beta(x_1, x_2) = \int_{-\infty}^{\infty}\int_{-\infty}^{\infty} \exp[i(R_1x_1 + R_2x_2)] dZ_\beta(R_1, R_2), \tag{27}$$

which is in the form

$$C_{\beta h_\beta}(\xi, \zeta) = <\beta(\xi) h_\beta(\zeta)>$$

$$= 2\sigma_y^2 \lambda_\beta J[\Theta_1(\frac{\xi_1}{\lambda_\beta}, \frac{\xi_2}{\lambda_\beta}) - \frac{\zeta_1}{\lambda_\beta}\Theta_2(\frac{\xi_1}{\lambda_\beta}, \frac{\xi_2}{\lambda_\beta}) + \frac{\zeta_2}{\lambda_\beta}\Theta_3(\frac{\xi_1}{\lambda_\beta}, \frac{\xi_2}{\lambda_\beta}) - \Theta_1(\frac{\rho_1}{\lambda_\beta}, \frac{\rho_2}{\lambda_\beta})]. \tag{28}$$

Substituting Eq. (20) into Eq. (22), it is found that the semivariogram of the head process has the following form

$$\gamma_{h_y}(\xi, \zeta) = \frac{1}{2}\sigma_y^2 \lambda_y^2 J^2 \{\frac{3}{8}\frac{\rho_1^2}{\lambda_y^2} + \frac{1}{8}\frac{\rho_2^2}{\lambda_y^2} + \Psi_1(\frac{\rho_1}{\lambda_y}, \frac{\rho_2}{\lambda_y}) + \frac{\rho_1}{\lambda_y}[-\frac{\xi_1}{\lambda_y}\Psi_2(\frac{\xi_1}{\lambda_y}, \frac{\xi_2}{\lambda_y}) + \frac{\zeta_1}{\lambda_y}\Psi_2(\frac{\zeta_1}{\lambda_y}, \frac{\zeta_2}{\lambda_y})]$$

$$+ \frac{\rho_2}{\lambda_y}[\frac{\xi_2}{\lambda_y}\Psi_3(\frac{\xi_1}{\lambda_y}, \frac{\xi_2}{\lambda_y}) - \frac{\zeta_2}{\lambda_y}\Psi_3(\frac{\zeta_1}{\lambda_y}, \frac{\zeta_2}{\lambda_y})]\}, \tag{29a}$$

$$\gamma_{h_\beta}(\xi, \zeta) = 2\sigma_\beta^2 \lambda_\beta^2 J^2 \{\frac{3}{8}\frac{\rho_1^2}{\lambda_\beta^2} + \frac{1}{8}\frac{\rho_2^2}{\lambda_\beta^2} + \Psi_1(\frac{\rho_1}{\lambda_\beta}, \frac{\rho_2}{\lambda_\beta}) + \frac{\rho_1}{\lambda_\beta}[-\frac{\xi_1}{\lambda_\beta}\Psi_2(\frac{\xi_1}{\lambda_\beta}, \frac{\xi_2}{\lambda_\beta}) + \frac{\zeta_1}{\lambda_\beta}\Psi_2(\frac{\zeta_1}{\lambda_\beta}, \frac{\zeta_2}{\lambda_\beta})]$$

$$+ \frac{\rho_2}{\lambda_\beta}[\frac{\xi_2}{\lambda_\beta}\Psi_3(\frac{\xi_1}{\lambda_\beta}, \frac{\xi_2}{\lambda_\beta}) - \frac{\zeta_2}{\lambda_\beta}\Psi_3(\frac{\zeta_1}{\lambda_\beta}, \frac{\zeta_2}{\lambda_\beta})]\}, \tag{29b}$$

https://doi.org/10.5194/hess-2022-298
Preprint. Discussion started: 17 October 2022
© Author(s) 2022. CC BY 4.0 License.

where $\rho_1 = \xi_1\text{-}\zeta_1$, $\rho_2 = \xi_2\text{-}\zeta_2$, and the description for the functions $\Psi_1\text{-}\Psi_3$, respectively, can be found in Appendix B.

In the case of statistically nonhomogeneous random fields, the structure of variability can be characterized by considering the semivariogram of a random field. If the semivariogram depends only on the separation, the random field is said to have stationary increments. The semivariogram in Eq. (29) clearly depends on the spatial location, which means that the processes of depth-averaged hydraulic head are nonstationary.

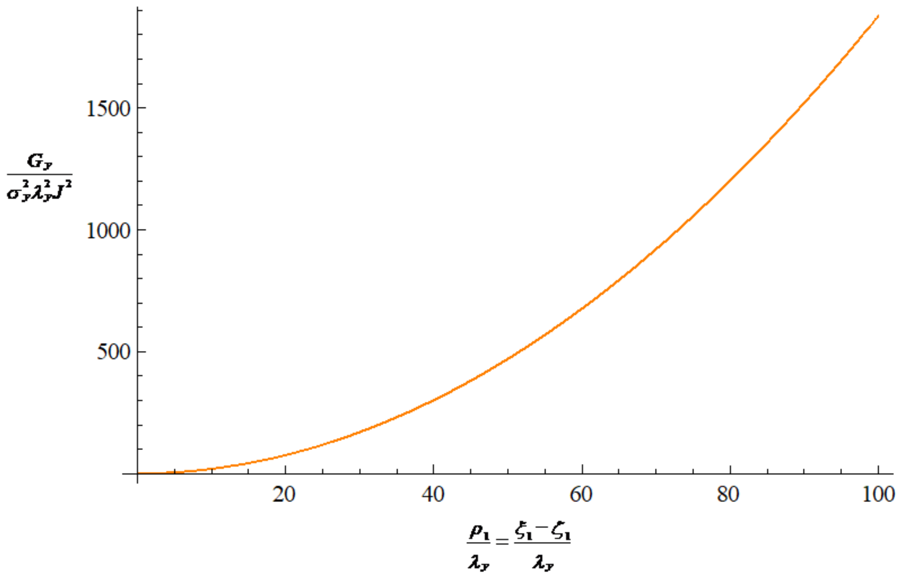

Figure 1. The stationary parts of the semivariogram of the head field, reflecting the effect of variation in the hydraulic conductivity fields, as a function of the separation distance in the mean flow direction, where G_y is the sum of the first three terms on the right-hand side of Eq. (29a).

https://doi.org/10.5194/hess-2022-298
Preprint. Discussion started: 17 October 2022
© Author(s) 2022. CC BY 4.0 License.

Figure 1 shows graphically the behavior of the stationary parts of the semivariogram (namely, the sum of the first three terms on the right-hand side of Eq. (29a)) as a function of the separation distance in the x_1-direction (mean flow direction). The semivariogram of the head field, reflecting the effect of variation in the hydraulic conductivity fields, shows an unlimited increase, as shown in Fig. 1. The unbounded head semivariogram suggests that there is no head covariance function (or the hydraulic head field with infinite variance). In this case, the use of the semivariogram is an appropriate way to measure the variability of the head variation. Similar conclusions can be drawn from Fig. 2, a graphical representation of the stationary parts of the semivariogram of the head field in Eq. (29b) in the mean flow direction, which reflects the effect of the variation of the aquifer thickness fields.

At this point, the covariance function for the depth-averaged velocity process in Eq. (21) can now be determined in conjunction with Eqs. (23), (26), (28), and (29). For example, the covariance of flow velocity for the separation along the mean flow direction is explicitly determined as follows:

$$< v_1(\xi_1,\xi_2) v_1(\zeta_1,\zeta_2=\xi_2) > = < v_{y_1}(\xi_1,\xi_2) v_{y_1}(\zeta_1,\xi_2) > + < v_{\beta_1}(\xi_1,\xi_2) v_{\beta_1}(\zeta_1,\xi_2) >, \tag{30a}$$

where

$$\frac{< v_{y_1}(\xi_1,\xi_2) v_{y_1}(\zeta_1,\xi_2) >}{V^2} = \sigma_y^2 \Big\{ \frac{3}{8} + \exp(-\frac{\rho}{\lambda_y}) - \Big[2\Xi_1(\frac{\rho_1}{\lambda_y},0) - \Xi_1(\frac{\xi_1}{\lambda_y},\frac{\xi_2}{\lambda_y}) - \Xi_1(\frac{\zeta_1}{\lambda_y},\frac{\xi_2}{\lambda_y}) \Big]$$

$$+ \Big[\Xi_2(\frac{\rho_1}{\lambda_y},0) - \Xi_2(\frac{\xi_1}{\lambda_y},\frac{\xi_2}{\lambda_y}) - \Xi_2(\frac{\zeta_1}{\lambda_y},\frac{\xi_2}{\lambda_y}) \Big] \Big\}, \tag{30b}$$

© Author(s) 2022. CC BY 4.0 License.

$$\frac{< v_{\beta_1}(\xi_1,\xi_2) v_{\beta_1}(\zeta_1,\xi_2) >}{V^2} = \sigma_\beta^2 \Big\{ \frac{3}{2} + \exp(-\frac{\rho}{\lambda_\beta}) - 2\Big[2\Xi_1(\frac{\rho_1}{\lambda_\beta},0) - \Xi_1(\frac{\xi_1}{\lambda_\beta},\frac{\xi_2}{\lambda_\beta}) - \Xi_1(\frac{\zeta_1}{\lambda_\beta},\frac{\xi_2}{\lambda_\beta}) \Big]$$

$$+4\Big[\Xi_2(\frac{\rho_1}{\lambda_\beta},0) - \Xi_2(\frac{\xi_1}{\lambda_\beta},\frac{\xi_2}{\lambda_\beta}) - \Xi_2(\frac{\zeta_1}{\lambda_\beta},\frac{\xi_2}{\lambda_\beta}) \Big] \Big\}, \tag{30c}$$

$\rho = (\rho_1^2 + \rho_2^2)^{1/2}$ and expressions for Ξ_1 and Ξ_2 are given, respectively, in the Appendix C. This should be used to compute the variance of solute displacement in the mean flow direction. The nonstationarity of the velocity covariance in Eq. (30) is evident in the dependence on spatial location, which is caused by nonstationarity in the hydraulic head processes.

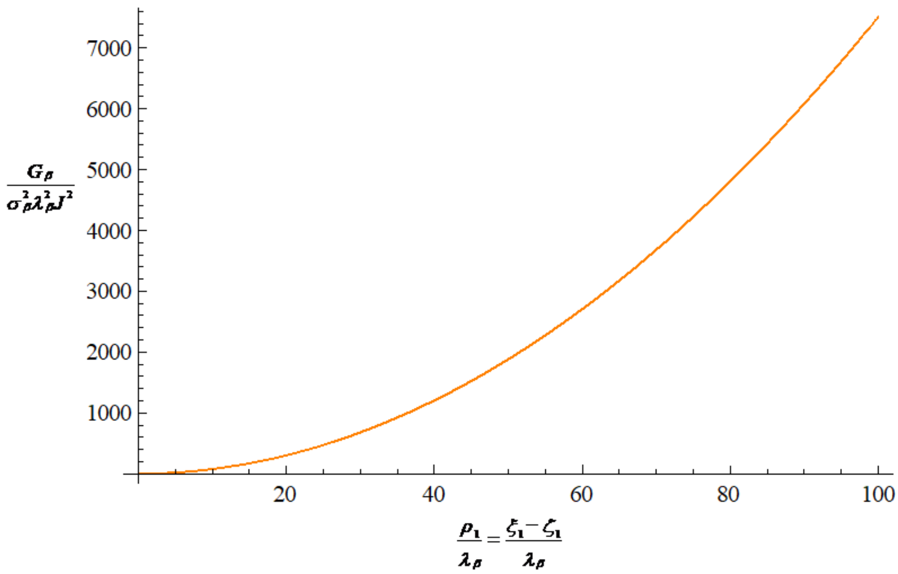

Figure 2. The stationary parts of the semivariogram of the head field, reflecting the effect of the variation of the aquifer thickness fields, as a function of the separation distance in the mean flow direction, where G_β is the sum of the first three terms on the right-hand side of Eq. (29b).

In the limit of $\zeta_1 \rightarrow \xi_1$, Eq. (30) approaches to the velocity variances in the mean

https://doi.org/10.5194/hess-2022-298
Preprint. Discussion started: 17 October 2022
© Author(s) 2022. CC BY 4.0 License.

flow direction as

$$\sigma_v^2 = \sigma_{v_y}^2(\xi_1,\xi_2) + \sigma_{v_\beta}^2(\xi_1,\xi_2), \tag{31a}$$

where

$$\frac{\sigma_{v_y}^2}{V^2\sigma_y^2} = \frac{1}{4}\frac{1}{\xi^8}\Delta_1\left(\frac{\xi_1}{\lambda_y},\frac{\xi_2}{\lambda_y}\right) + \frac{1}{4}\frac{1}{\xi^9}\exp\left[-\frac{\xi}{\lambda_y}\right]\Delta_2\left(\frac{\xi_1}{\lambda_y},\frac{\xi_2}{\lambda_y}\right), \tag{31b}$$

$$\frac{\sigma_{v_\beta}^2}{V^2\sigma_\beta^2} = \frac{1}{2}\frac{1}{\xi^8}\Delta_3\left(\frac{\xi_1}{\lambda_\beta},\frac{\xi_2}{\lambda_y}\right) + \frac{1}{2}\frac{1}{\xi^9}\exp\left[-\frac{\xi}{\lambda_\beta}\right]\Delta_4\left(\frac{\xi_1}{\lambda_\beta},\frac{\xi_2}{\lambda_\beta}\right). \tag{31c}$$

where $\xi = (\xi_1^2+\xi_2^2)^{1/2}$ and expressions for Δ_1-Δ_4 are given, respectively, in the Appendix D. From equation (31), it can be seen that the variance of the flow velocity is positively correlated with the variances of the log-hydraulic conductivity and log-aquifer thickness. This means that the variability of the flow velocity field increases with the variability of the hydraulic conductivity and aquifer thickness fields.

4.2 Variance of the solute displacement in the mean flow direction

The stochastic Eq. (16) is more complex because the first term appears on the right-hand side of Eq. (16). In general, it is not possible to explicitly derive the relationships between the variance of solute displacement and that of the flow field using the solution of Eq. (16). To take advantage of the closed form, this study considers the case where the local dispersivity is very small compared to the integral

https://doi.org/10.5194/hess-2022-298
Preprint. Discussion started: 17 October 2022
© Author(s) 2022. CC BY 4.0 License.
Hydrology and Earth System Sciences
Discussions

scales for the ln$K$ and ln$B$ processes, so that the solute dispersion is mainly caused by the spatial variability of hydraulic conductivity and thickness of confined aquifer. That is, solute dispersion occurs in situations where advection dominates and solute particles do not transfer across streamlines. There are numerous studies in the literature on solute transport under advection-dominated conditions, e.g., Dagan (1984), Rubin and Bellin (1994), Butera et al. (2009), Cvetkovic (2016), Ciriello and Barros (2020), etc.

In advection-dominated situations, the local dispersion coefficient D_L in Eq. (16) can be set to zero and Eq. (16) is simplified to

$$\frac{dX_1^{'}}{dt} = v_1(<\mathbf{X}>), \tag{32}$$

which gives the solution

$$X_1^{'}(t) = \int_0^t v_1(VS, 0)dS \,. \tag{33}$$

This implies that the displacement variance can be expressed in terms of the flow velocity covariance through the double integral as

$$X_{11}(t) = \int_0^t \int_0^t < v_1(VS_1, 0) v_1(VS_2, 0) > dS_1 dS_2 \,. \tag{34}$$

4.2.1 Nonstationary flow fields

https://doi.org/10.5194/hess-2022-298
Preprint. Discussion started: 17 October 2022
© Author(s) 2022. CC BY 4.0 License.

Hydrology and Earth System Sciences
Open Access
EGU
Discussions

Substituting Eq. (30) into Eq. (34) and integrating it with $\xi_2 = 0$ yields the following expression for the variance of longitudinal solute displacement as

$$X_{11}(t) = X_{11_y}(t) + X_{11_\beta}(t) , \tag{35a}$$

where

$$\frac{X_{11_y}(t)}{\sigma_y^2 \lambda_y^2} = \frac{5}{2} - 3\gamma - \frac{9}{\Gamma^2} + 2\Gamma + \frac{3}{8}\Gamma^2 + 3Ei(-\Gamma) - 3\ln(\Gamma) + e^{-\Gamma}\left(2 + \frac{9}{\Gamma^2} + \frac{9}{\Gamma}\right), \tag{35b}$$

$$\frac{X_{11_\beta}(t)}{\sigma_\beta^2 \lambda_\beta^2} = 4 - 4\gamma - \frac{36}{\vartheta^2} + 2\vartheta + \frac{3}{2}\vartheta^2 + 4Ei(-\vartheta) - 4\ln(\vartheta) + 2e^{-\vartheta}\left(7 + 2\vartheta + \frac{18}{\vartheta^2} + \frac{18}{\vartheta}\right), \tag{35c}$$

$\Gamma = Vt/\lambda_y$, and $\vartheta = Vt/\lambda_\beta$.

4.2.2 Stationary flow fields

Gutjahr and Gelhar (1981) show that the Poission equation in an unbounded porous medium such as equation (19a) also has a zero-order intrinsic random function (0-IRF) as its solution when the input random process has a finite variance. That is, Eqs. (19a) and (19b) with stationary processes y and β admit the solutions of the form

$$h_y(x_1, x_2) = J \int_{-\infty}^{\infty}\int_{-\infty}^{\infty} iR_1 \frac{1 - \exp[i(R_1 x_1 + R_2 x_2)]}{R_1^2 + R_2^2} dZ_y(R_1, R_2) , \tag{36a}$$

$$h_\beta(x_1, x_2) = 2J \int_{-\infty}^{\infty}\int_{-\infty}^{\infty} iR_1 \frac{1 - \exp[i(R_1 x_1 + R_2 x_2)]}{R_1^2 + R_2^2} dZ_\beta(R_1, R_2) . \tag{36b}$$

https://doi.org/10.5194/hess-2022-298
Preprint. Discussion started: 17 October 2022
© Author(s) 2022. CC BY 4.0 License.

Using a similar methodology as above and based on Eq. (36), one would arrive at the following results

$$C_{yh_y}(\xi,\zeta)=\sigma_y^2\lambda_y J\left[\Theta_1\left(\frac{\xi_1}{\lambda_y},\frac{\xi_2}{\lambda_y}\right)-\Theta_1\left(\frac{\rho_1}{\lambda_y},\frac{\rho_2}{\lambda_y}\right)\right], \tag{37a}$$

$$C_{yh_y}(\xi,\zeta)=\sigma_y^2\lambda_y J\left[\Theta_1\left(\frac{\xi_1}{\lambda_y},\frac{\xi_2}{\lambda_y}\right)-\Theta_1\left(\frac{\rho_1}{\lambda_y},\frac{\rho_2}{\lambda_y}\right)\right], \tag{37b}$$

$$\gamma_{h_y}(\xi,\zeta)=\frac{1}{2}\sigma_y^2\lambda_y^2 J^2\Psi_1\left(\frac{\rho_1}{\lambda_y},\frac{\rho_2}{\lambda_y}\right), \tag{38a}$$

$$\gamma_{h_\beta}(\xi,\zeta)=2\sigma_\beta^2\lambda_\beta^2 J^2\Psi_1\left(\frac{\rho_1}{\lambda_\beta},\frac{\rho_2}{\lambda_\beta}\right), \tag{38b}$$

from which it follows that in the mean flow direction,

$$<v_1(\xi_1,\xi_2)v_1(\zeta_1,\zeta_2=\xi_2)>=<v_{y_1}(\xi_1,\xi_2)v_{y_1}(\zeta_1,\xi_2)>+<v_{\beta_1}(\xi_1,\xi_2)v_{\beta_1}(\zeta_1,\xi_2)>, \tag{39a}$$

where

$$\frac{<v_{y_1}(\xi_1,\xi_2)v_{y_1}(\zeta_1,\xi_2)>}{V^2}=\sigma_y^2\left[\frac{3}{2}\left(-\frac{6}{\varphi^4}+\frac{1}{\varphi^2}\right)+3e^{-\varphi}\left(\frac{3}{\varphi^4}+\frac{3}{\varphi^3}+\frac{1}{\varphi^2}\right)\right], \tag{39b}$$

$$\frac{<v_{\beta_1}(\xi_1,\xi_2)v_{\beta_1}(\zeta_1,\xi_2)>}{V^2}=\sigma_\beta^2\left[-2\left(\frac{18}{\upsilon^4}+\frac{1}{\upsilon^2}\right)+e^{-\varphi}\left(1+\frac{36}{\upsilon^4}+\frac{36}{\upsilon^3}+\frac{16}{\upsilon^2}+\frac{4}{\upsilon}\right)\right], \tag{39c}$$

$\varphi = (\xi_1\text{-}\zeta_1)/\lambda_y$ and $\upsilon = (\xi_1\text{-}\zeta_1)/\lambda_\beta$. Finally, the variance of solute displacement in the mean flow direction is obtained from Eq. (34) by applying Eq. (39):

$$X_{11}(t)=X_{11_y}(t)+X_{11_\beta}(t), \tag{40a}$$

where

$$\frac{X_{11_y}(t)}{\sigma_y^2\lambda_y^2}=\frac{3}{2}-3\gamma+2\Gamma-\frac{3}{\Gamma^2}+3Ei(-\Gamma)-3\ln(\Gamma)+3e^{-\Gamma}\left(\frac{1}{\Gamma^2}+\frac{1}{\Gamma}\right), \tag{40b}$$

$$\frac{X_{11_\beta}(t)}{\sigma_\beta^2\lambda_\beta^2}=4-4\gamma-\frac{12}{\vartheta^2}+2\vartheta+4Ei(-\vartheta)-4\ln(\vartheta)+2e^{-\vartheta}\left(1+\frac{6}{\vartheta^2}+\frac{6}{\vartheta}\right). \tag{40c}$$

Equation (40b) is equivalent to the solution of Dagan (1982; 1984) using the Green function approach, where the variance and integral scale of the log conductivity fields

https://doi.org/10.5194/hess-2022-298
Preprint. Discussion started: 17 October 2022
© Author(s) 2022. CC BY 4.0 License.
Hydrology and Earth System Sciences
Open Access
Discussions

in Eq. (40b) are replaced by the variance and integral scale of the log transmissivity fields.

A comparison of the prediction of the solute longitudinal displacement variance in Eq. (35b) in nonstationary flow fields with the prediction in Eq. (40b) in stationary flow fields is shown graphically in Fig. 3. The variance of the longitudinal displacement in response to the change in the hydraulic conductivity grows monotonically with travel time. It can also be seen that the difference in displacement variance caused by the nonstationary and stationary flow fields increases with travel time, which means that the longitudinal mscrodispersion in nonstationary flow fields becomes anomalous and a Fick's regime is not achieved. This behavior of anomalous macrodispersion is attributed to the effect of nonstationary hydraulic head fields caused by the variation of hydraulic conductivity.

A macrodispersion coefficient in the mean flow direction can be defined by half of the time derivative of Eq. (35b) as follows:

$$D_{11_y}(t)=\sigma_y^2\lambda_y V\left[1+\frac{9}{\Gamma^3}-\frac{3}{2}\frac{1}{\Gamma}+\frac{3}{8}\Gamma-e^{-\Gamma}\left(1+\frac{9}{\Gamma^3}+\frac{9}{\Gamma^2}+\frac{3}{\Gamma}\right)\right]. \tag{41a}$$

This implies that the longitudinal macrodispersion coefficient at large time in nonstationary flow fields can be approximated as

$$D_{11_y}(t)\approx\sigma_y^2\lambda_y V\left(1+\frac{3}{8}\Gamma\right). \tag{41b}$$

That is, the longitudinal macrodispersion increases linearly with travel time at large

https://doi.org/10.5194/hess-2022-298
Preprint. Discussion started: 17 October 2022
© Author(s) 2022. CC BY 4.0 License.

distances. Note that, in stationary flow fields, the longitudinal macrodispersion coefficient approaches an asymptotic limit $D_{11_y} = \sigma_y^2 \lambda_y V$ at large time. Clearly, applying the asymptotic macrodispersion coefficient (Eq. (41b)), which is appropriate for macrodispersion in stationary flow fields, to the prediction of macrodispersion in the downstream region at a large distance from the contamination source leads to a significant underestimation of macrodispersion in nonstationary flow fields.

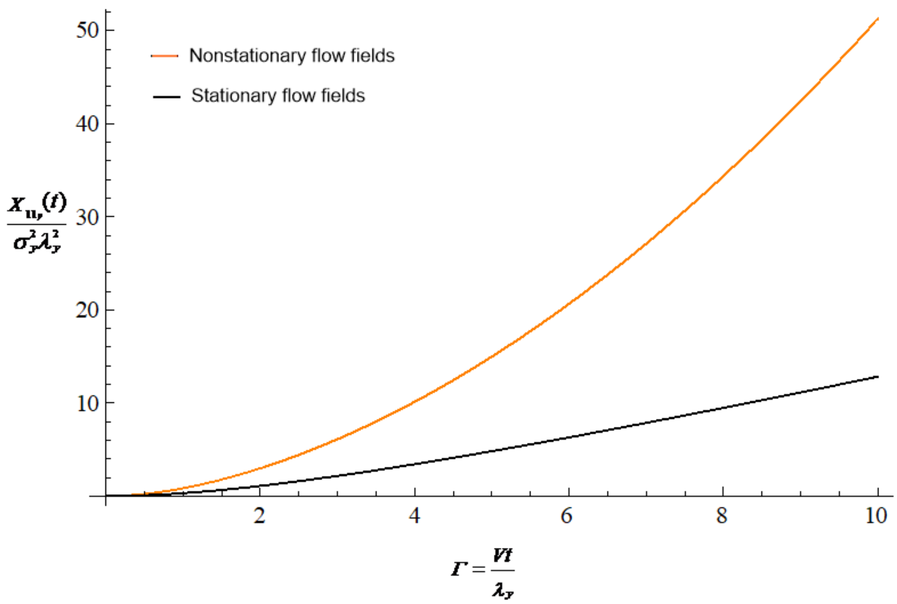

Figure 3. Comparison of the prediction of the solute longitudinal displacement variance in Eq. (35b) in nonstationary flow fields with the prediction in Eq. (40b) in stationary flow fields.

The behavior of the longitudinal displacement variance of solutes, affected by the effect of variation of aquifer thickness field, in the nonstationary flow field (Eq. (35c))

https://doi.org/10.5194/hess-2022-298
Preprint. Discussion started: 17 October 2022
© Author(s) 2022. CC BY 4.0 License.
Hydrology and Earth System Sciences Open Access EGU Discussions

and in the stationary flow field (Eq. (40c)) as a function of travel time is also presented graphically in Fig. 4. This again demonstrates that the displacement variance grows faster than linear with travel time and the longitudinal macrodispersion becomes anomalous at large travel times. The corresponding longitudinal macrodispersion coefficient is

$$D_{11_\beta}(t)=\sigma_\beta^2\lambda_\beta V\left[1+\frac{36}{\vartheta^3}-\frac{2}{\vartheta}+\frac{3}{2}\vartheta-e^{-\vartheta}\left(5+\frac{36}{\vartheta^3}+\frac{36}{\vartheta^2}+\frac{16}{\vartheta}+2\vartheta\right)\right], \quad (42a)$$

with the approximation at large times as

$$D_{11_\beta}(t)\approx\sigma_\beta^2\lambda_\beta V\left(1+\frac{3}{2}\vartheta\right). \quad (42b)$$

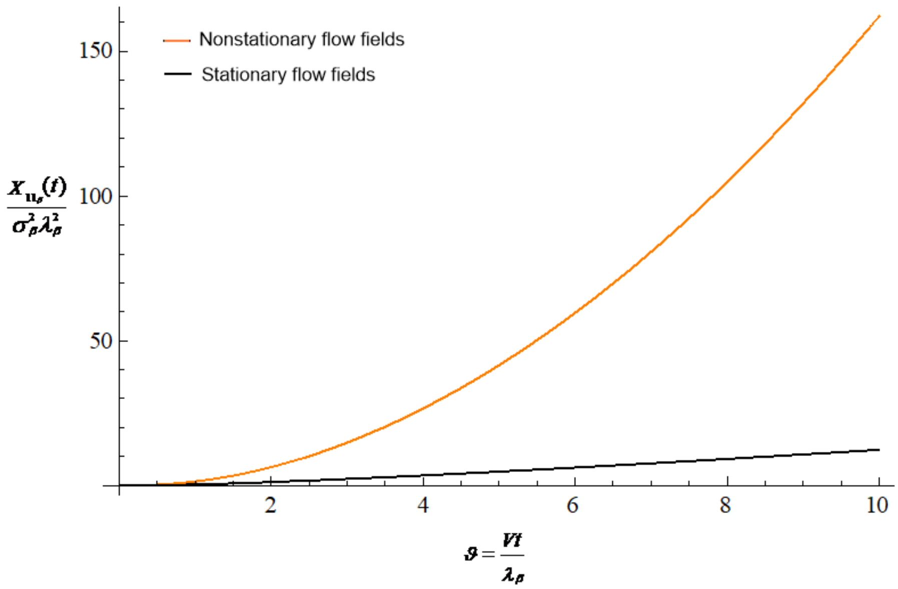

Figure 4. Comparison of the prediction of the solute longitudinal displacement variance in Eq. (35c) in nonstationary flow fields with the prediction in Eq. (40c) in stationary flow fields.

© Author(s) 2022. CC BY 4.0 License.

5 Conclusions

In this work, a theoretical stochastic methodology is developed to quantify the displacement variance of an inert solute particle in heterogeneous confined aquifers with variable thickness. This methodology relates solute displacement to the Fokker-Planck equation through the two-dimensional depth-averaged solute mass conservation equation. In contrast to previous stochastic studies of two-dimensional solute transport problems, the variability of solute movement is caused not only by the variability of log conductivity, but also by the variability of log thickness of confined aquifer.

The two-dimensional stochastic groundwater flow equation for the depth-averaged hydraulic head perturbation always has a 1-IRF solution when the log hydraulic conductivity and log aquifer thickness fields are second-order stationary. This leads to an unbounded increasing head semivariogram where no head covariance exists. The nonstationarity of the hydraulic head leads to nonstationary flow velocity fields and thus a nonlinear increase in longitudinal solute displacement with travel time. That is, a Fick's regime is not achieved, and the longitudinal macrodispersion becomes anomalous and increases linearly with travel time at large distances. It is also

https://doi.org/10.5194/hess-2022-298
Preprint. Discussion started: 17 October 2022
© Author(s) 2022. CC BY 4.0 License.
Hydrology and Earth System Sciences
Discussions

shown that the variability of solute displacement in the mean flow direction increases with the variability of hydraulic conductivity and aquifer thickness.

Appendix A: Expressions for the functions in Eqs. (26) and (28)

$$\Theta_1(a,b)=\frac{a}{r}[1-e^{-r}(1+r)], \tag{A1}$$

$$\Theta_2(a,b)=-2\frac{a^2}{r^4}+\frac{1}{r^2}+e^{-r}[a^2(\frac{2}{r^4}+\frac{2}{r^3}+\frac{1}{r^2})-\frac{1}{r^2}-\frac{1}{r}], \tag{A2}$$

$$\Theta_3(a,b)=ab[\frac{2}{r^4}-e^{-r}(\frac{2}{r^4}+\frac{2}{r^3}+\frac{1}{r^2})], \tag{A3}$$

where $r^2 = a^2+b^2$.

Appendix B: Expressions for the functions in Eq. (29)

$$\Psi_1(a,b)=\frac{a^2-b^2}{r^2}[\frac{1}{2}+\frac{e^{-r}(r^2+3r+3)-3}{r^2}]-Ei(r)+\ln(r)+e^{-r}-1+\gamma, \tag{B1}$$

$$\begin{aligned}\Psi_2(a,b)=&\frac{1}{r^6}(a^4+6a^2+4a^2b^2+3b^4-18b^2)+e^{-r}[-2\frac{a^6}{r^7}-a^4(\frac{6}{r^7}+\frac{4}{r^6})-6\frac{a^2}{r^6}-4\frac{a^4b^2}{r^7}\\&+2a^2b^2(\frac{6}{r^7}+\frac{1}{r^6})-2\frac{a^2b^4}{r^7}+6b^4(\frac{3}{r^7}+\frac{1}{r^6})+18\frac{b^2}{r^6}],\end{aligned} \tag{B2}$$

$$\begin{aligned}\Psi_3(a,b)=&\frac{1}{r^6}(a^4-18a^2-b^4+6b^2)+e^{-r}[2\frac{a^6}{r^7}+2a^4(\frac{9}{r^7}+\frac{4}{r^6})+18\frac{a^2}{r^6}+4\frac{a^4b^2}{r^7}\\&+2\frac{a^2b^4}{r^7}+6a^2b^2(\frac{2}{r^7}+\frac{1}{r^6})-2b^4(\frac{3}{r^7}+\frac{1}{r^6})-6\frac{b^2}{r^6}],\end{aligned} \tag{B3}$$

where $r^2 = a^2+b^2$, Ei is the exponential integral, and γ is the Euler constant.

https://doi.org/10.5194/hess-2022-298
Preprint. Discussion started: 17 October 2022
© Author(s) 2022. CC BY 4.0 License.

Appendix C: Expressions for the functions in Eq. (30)

$$\Xi_1(a,b) = -2\frac{9}{r^4} + \frac{1}{r^2} + e^{-r}\left[a^2\left(\frac{2}{r^4} + \frac{2}{r^3} + \frac{1}{r^2}\right) - \frac{1}{r^2} - \frac{1}{r}\right], \quad \text{(C1)}$$

$$\Xi_2(a,b) = -\frac{1}{2}\frac{1}{r^8}\Omega_1 + \frac{e^{-r}}{r^9}\Omega_2 + \frac{e^{-r}}{r^8}\Omega_3, \quad \text{(C2)}$$

where $r = (a^2+b^2)^{1/2}$,

$$\Omega_1(a,b) = a^6 + 3a^2b^2(-36+b^2) - 3b^4(-6+b^2) + a^4(18+7b^2), \quad \text{(C3)}$$

$$\Omega_2(a,b) = 2a^8 + 9b^6 + a^6(9-2b^2) - 5a^4b^2(9+2b^2) - 3a^2b^4(15+2b^2), \quad \text{(C4)}$$

$$\Omega_3(a,b) = a^8 + 3b^4(3+b^2) + a^6(5+2b^2) - 3a^2b^2(18+7b^2) + b^4(9-19b^2+b^4), \quad \text{(C5)}$$

Appendix D: Expressions for the functions in Eq. (31)

$$\Delta_1(a,b) = 3a^8 + 4a^6(-1+3b^2) + b^4(72-4b^2+3b^4) + 4a^2b^4(-108+5b^2+3b^4) + 2a^4(36+10b^2+9b^4), \quad \text{(D1)}$$

$$\Delta_2(a,b) = -8a^8 + 4a^6[-18-8r+(8+2r)3b^2] + b^4[-72r-4(8+8r)b^2-8b^4]$$
$$+4a^2b^2[108r+5(18+8r)b^2+(8+2r)b^4] + 2a^4[-36r+10(18+8r)b^2+(40+8r)b^4], \quad \text{(D2)}$$

$$\Delta_3(a,b) = a^8 + 4a^6b^2 + b^4(144-16b^2+b^4) + 4a^2b^4(-216+8b^2+b^4) + 6a^4(24+8b^2+b^4), \quad \text{(D3)}$$

$$\Delta_4(a,b) = -8(3+r)a^8 + 4a^6[-18(2+r)+(12-2r)b^2] + b^4[-144r-8(18+7r)b^2-8b^4]$$
$$+4a^2b^2[216r+2(90+41r)b^2+(20+2r)b^4] + 2a^4[-72r+12(30+13r)b^2+(80+4r)b^4], \quad \text{(D4)}$$

where $r = (a^2+b^2)^{1/2}$.

https://doi.org/10.5194/hess-2022-298
Preprint. Discussion started: 17 October 2022
© Author(s) 2022. CC BY 4.0 License.

Data availability. No data was used for the research described in the article.

Author contributions. C-MC: Conceptualization, Methodology, Formal analysis, Writing - original draft preparation, Writing - review & editing.
C-FN: Conceptualization, Methodology, Formal analysis, Writing - original draft preparation, Writing - review & editing, Supervision, Funding acquisition.
C-PL: Conceptualization, Methodology, Formal analysis, Writing - original draft preparation, Writing - review & editing.
I-HL: Conceptualization, Methodology, Formal analysis, Writing - original draft preparation, Writing - review & editing.

Competing interests. The authors declare that they have no conflict of interest.

Acknowledgements. Research leading to this paper has been partially supported by the grant from the Taiwan Ministry of Science and Technology under the grants MOST 108-2638-E-008-001-MY2, MOST 110-2123-M-008-001-, MOST 110-2621-M-008-003-, and MOST 110-2811-M-008-533.

References

Bailey, R. T. and Baù, D.: Estimating geostatistical parameters and spatially-variable hydraulic conductivity within a catchment system using an ensemble smoother,

https://doi.org/10.5194/hess-2022-298
Preprint. Discussion started: 17 October 2022
© Author(s) 2022. CC BY 4.0 License.

Hydrol. Earth Syst. Sci., 16(2), 287-304, 2012.

Bear, J.: Hydraulics of groundwater, McGraw-Hill, New York, 1979.

Bear, J. and Cheng, A.H.-D.: Modeling groundwater flow and contaminant transport, Springer, Dordrecht, 2010.

Butera I. and Tanda, M.: Solute transport analysis through heterogeneous media in nonuniform in the average flow by a stochastic approach, Transp. Porous Media, 36(3), 255-291, 1999.

Butera, I., Cotto, I., and Ostorero, V.: A geostatistical approach to the estimation of a solute trajectory through porous formations, J. Hydrol., 375(3-4), 345-355, 2009.

Chang, C-M, Ni, C-F, Li, W-C, Lin, C-P, and Lee, I-H: Stochastic analysis of the variability of groundwater flow fields in heterogeneous confined aquifers of variable thickness, Stoch. Environ. Res. Risk Assess., https://doi.org/10.1007/s00477-021-02125-7, 2021.

Chile`s, J. P. and Delfiner, P.: Geostatistics: modeling spatial uncertainty, 1st ed., Wiley-Interscience, New York, 1999.

Ciriello, V. and Barros, F. P. J.: Characterizing the influence of multiple uncertainties on predictions of contaminant discharge in groundwater within a Lagrangian stochastic formulation, Water Resour. Res., 56(10), doi:10.1029/2020wr027867, 2020.

https://doi.org/10.5194/hess-2022-298
Preprint. Discussion started: 17 October 2022
© Author(s) 2022. CC BY 4.0 License.
Hydrology and Earth System Sciences
Open Access
Discussions

Cuello, J. E. and Guarracino, L.: Tide-induced head fluctuations in coastal aquifers of variable thickness, Hydrol. Process., 34, 4139-4146, 2020.

Cvetkovic, V., Fiori, A., and Dagan, G.: Tracer travel and residence time distributions in highly heterogeneous aquifers: Coupled effect of flow variability and mass transfer, J. Hydrol., 543(Part A), 101-108, 2016.

Dagan, G.: Stochastic modeling of groundwater flow by unconditional and conditional probabilities: 2. The solute transport, Water Resour. Res., 18(4), 835-848, 1982.

Dagan, G.: Solute transport in heterogeneous porous formation, J. Fluid Mech., 145, 151-177, 1984.

Dagan, G.: Flow and transport in porous formations, Springer, New York, 1989.

de Marsily, G.: Quantitative hydrogeology: Groundwater hydrology for engineers, Academic Press, Orlando, FL, 1986.

DeSimone, L. A., Pope, J. P., and Ransom, K. M.: Machine-learning models to map pH and redox conditions in groundwater in a layered aquifer system, Northern Atlantic Coastal Plain, eastern USA, J. Hydrol. Reg. Stud., 30, 100697, 2020.

Fischer, H. B., List, E. J., Koh, R., Imberger, J., and Brooks, N.: Mixing in inland and coastal waters, Academic, San Diego, 1979.

Gelhar, L. W.: Stochastic Subsurface Hydrology, Prentice Hall, Englewood Cliffs, New Jersey, 1993.

© Author(s) 2022. CC BY 4.0 License.

Guadagnini, A. and Neuman, S. P.: Nonlocal and localized analyses of conditional mean steady state flow in bounded, randomly nonuniform domains: 2. Computational examples, Water Resour. Res., 35, 3019-3039, 1999.

Gutjahr, A. L. and Gelhar, L. W.: Stochastic models of subsurface flow: infinite versus finite domains and stationarity, Water Resour. Res., 17(2), 337-350, 1981.

Hantush, M. S.: Flow of ground water in sands of nonuniform thickness, part 3. Flow to wells, J. Geophys. Res., 67(4), 1527-1534, 1962.

Holly, F. M. JR.: Two-dimensional mass dispersion in rivers, Hydrology Papers, No. 78., Colorado State University, Fort Collins, 1975.

Jing, M., Heße, F., Kumar, R., Kolditz, O., Kalbacher, T., and Attinger, S.: Influence of input and parameter uncertainty on the prediction of catchment-scale groundwater travel time distributions, Hydrol. Earth Syst. Sci., 23(1), 171-190, 2019.

Lumley J. L. and Panofsky, H. A.: The structure of atmospheric turbulence, John Wiley, New York, 1964.

Masterson, J. P, Pope, J. P., Monti, J., Nardi, M. R., Finkelstein, J. S., and McCoy, K. J.: Hydrogeology and hydrologic conditions of the Northern Atlantic Coastal Plain aquifer system from Long Island, New York, to North Carolina, US Geol. Surv. Sci. Invest Rep., 2013-5133, 2013.

© Author(s) 2022. CC BY 4.0 License.

Matheron, G.: The intrinsic random functions and their applications, Adv. Appl. Probab., 5(3), 439-468, 1973.

Risken, H.: The Fokker-Planck equation, Springer, New York, 1989.

Rubin, Y. and Bellin, A.: The effects of recharge on flow nonuniformity and macrodispersion, Water Resour. Res., 30(4), 939-948, 1994.

Rubin, Y.: Applied Stochastic Hydrogeology, Oxford University Press, New York, 2003.

Van Kampen, N. G.: Stochastic processes in physics and chemistry, North-Holland, Amsterdam, 1992.

Zamrsky, D., Oude Essink, G. H., and Bierkens, M. F.: Estimating the thickness of unconsolidated coastal aquifers along the global coastline, Earth Syst. Sci. Data, 10(3), 1591-1603, 2018.

Zhang, D. and Winter, C. L.: Moment equation approach to single phase fluid flow in heterogeneous reservoirs, Soc. Petrol Eng. J., 4, 118-127, 1999.